NPS-EC-97-006

NAVAL POSTGRADUATE SCHOOL
Monterey, California

EMI Leakage into the Radio Frequency Distribution System of a Receiving Site

by

Wilbur R. Vincent
Richard W. Adler
Hugh J. Myers

January 1997

Approved for public release; distribution unlimited.

Prepared for: COMNAVSECGRU, N-44

NAVAL POSTGRADUATE SCHOOL
Monterey, California

Rear Admiral M.J. Evans
Superintendent

R. Elster
Provost

This report was prepared for and sponsored by COMNAVSECGRU, N44.

Approved for public release; distribution unlimited.

The report was prepared by:

WILBUR R. VINCENT
Research Associate Professor
Department of Electrical and
Computer Engineering

RICHARD W. ADLER
Senior Lecturer
Department of Electrical and
Computer Engineering

Reviewed by:

HERSCHEL H. LOOMIS, JR.
Chairman
Department of Electrical and
Computer Engineering

Released by:

DAVID W. NETZER
Associate Provost and
Dean of Research

REPORT DOCUMENTATION PAGE

Form Approved
OMB No. 0704-0188

1. AGENCY USE ONLY (Leave blank)	2. REPORT DATE	3. REPORT TYPE AND DATES COVERED
	January 1997	Technical Report

4. TITLE AND SUBTITLE
EMI Leakage into the Radio Frequency Distribution System of a Receiving Site

5. FUNDING NUMBERS
N00069-97-P0-75028

6. AUTHOR(S)
*Wilbur R. Vincent and Richard W. Adler
**Hugh J. Myers

7. PERFORMING ORGANIZATION NAME(S) AND ADDRESS(ES)
* Department of Electrical and Computer Engineering
Naval Postgraduate School, Monterey, CA 93943
** NRaD Activity Pacific, 675 Lehua Ave., Pearl City, HI 96782

8. PERFORMING ORGANIZATION REPORT NUMBER
NPS-EC-97-006

9. SPONSORING/MONITORING AGENCY NAME(S) AND ADDRESS(ES)
Headquarters Naval Security Group
Attn: Mrs. Jackie Sherry, N-44
9800 Savage Road
Ft. George G. Meade, MD 20755-6000

10. SPONSORING/MONITORING AGENCY REPORT NUMBER

11. SUPPLEMENTARY NOTES
The views expressed in this report are those of the author and do not reflect the official policy or position of the Department of Defense or the United States Government.

12a. DISTRIBUTION/AVAILABILITY STATEMENT
Approved for public release; distribution unlimited.

12b. DISTRIBUTION CODE
A

13. ABSTRACT (Maximum 200 words)

Test signals were injected into the shields of cables, ground conductors, and power conductors. The leakage of the test signals into the radio signal paths to receivers was explored. The maximum tolerable level of EMI current on shields, grounds, and power conductors was then determined. This information is useful in establishing the maximum permissible levels of EMI current on the conductors of a receiving site.

14. SUBJECT TERMS
radio noise, man-made noise, EMI/RFI, electromagnetic interference, radio frequency interference

15. NUMBER OF PAGES
43

16. PRICE CODE

17. SECURITY CLASSIFICATION OF REPORT	18. SECURITY CLASSIFICATION OF THIS PAGE	19. SECURITY CLASSIFICATION OF ABSTRACT	20. LIMITATION OF ABSTRACT
UNCLASSIFIED	UNCLASSIFIED	UNCLASSIFIED	SAR

PREFACE

This is the first technical report to be produced from an extensive examination of the isolation of the RF-Distribution (RFD) System of a CDAA site from site-generated conducted EMI. The work was done by a special Signal-to-Noise Enhancement Program (SNEP) team at the Wahiawa CDAA site operated by the Naval Security Group Department, Honolulu, Hawaii. Technical and administrative support was provided by NRaD Activity Pacific. The impetus for the work came from the observation of a large number of instances of site-generated interference leaking into RF paths and appearing as harmful levels of radio interference at the input to receivers.

Test signals were injected onto the shields of cables, ground conductors and power conductors, and the leakage of the test signals into signal paths to receiving systems was explored. The maximum tolerable level of current injected into these conductors to avoid harmful interference at the input to receivers was then determined. The levels of EMI current normally found on the conductors of today's receiving sites are often considerably higher than the tolerable levels.

Two solutions to the problem are identified. They are (1) the careful design and implementation of RFD systems to provide the greatest possible isolation from harmful levels of EMI current, and (2) the reduction of the present harmful levels of EMI current to harmless levels. A third, often proposed solution—better equipment and system grounding—is not an effective solution.

The authors of this report are especially grateful for the excellent assistance of all team members. Personnel of NRaD Activity Pacific and the staff of NSGD Honolulu were especially helpful in implementing this effort. Both organizations assisted in key aspects of the work, and they were essential to obtain the data used to produce this report. The findings of the effort have uncovered several problems in the design and construction techniques used in present-day receiving sites which need attention. The findings identify a key reason for the decline in the signal-intercept productivity of many of our receiving sites.

CONTENTS

PREFACE i
CONTENTS ii
LIST OF FIGURES iii
LIST OF TABLES iii

1. INTRODUCTION 1

2. BACKGROUND COMMENTS 2

3. IMPLEMENTATION 7
3.1 Instrumentation 7
3.2 EMI Leakage, Initial Test 9
3.3 EMI Leakage, Test 1 11
3.4 EMI Leakage, Test 2 14
3.5 EMI Leakage, Test 3 17
3.6 EMI Leakage, Test 4 20
3.7 EMI Leakage, Test 5 23

4. DISCUSSION 26
4.1 General Comments 26
4.2 Summary of Measured Leakage 28
4.3 Transfer Impedance 29
4.4 Corrective Actions 30
4.5 Other Conbsiderations 31

5. CONCLUSIONS 32

Appendix A PERSONNEL 33

INITIAL DISTRIBUTION LIST 35

LIST OF FIGURES

2-1 Example of the Adverse Impact of Site-Generated EMI on Signal Reception at a Large Site 3

2-2 Example of the Adverse Impact of Site-Generated EMI on Signal Reception at a Small Site 4

2-3 Example of the Adverse Impact of Site-Generated EMI on Signal Reception at a VHF/UHF Site 6

3.1-1 Injection Instrumentation 7

3.1-2 Signal Leakage Measurement Instrumentation 8

3.2-1 EMI Leakage from Initial Test 9

3.3-1 Block Diagram for Test 1 11

3.3-2 Low-Band EMI Leakage, Test 1 12

3.3-3 High-Band EMI Leakage, Test 1 13

3.4-1 Block Diagram for Test 2 14

3.4-2 Low-Band EMI Leakage, Test 2 15

3.4-3 High-Band EMI Leakage, Test 2 16

3.5-1 Block Diagram for Test 3 17

3.5-2 Low-Band EMI Leakage, Test 3 18

3.5-3 High-Band EMI Leakage, Test 3 19

3.6-1 Block Diagram for Test 4 20

3.6-2 Low-Band EMI Leakage, Test 4 21

3.6-3 High-Band EMI Leakage, Test 4 22

3.7-1 Block Diagram for Test 5 23

3.7-2 Low-Band EMI Leakage, Test 5 24

3.7-3 High-Band EMI Leakage, Test 5 25

LIST OF TABLES

4.2-1 Summary of Tolerable Levels of Discrete Frequency EMI Current 28

1. INTRODUCTION

A Signal-to-Noise-Enhancement Program (SNEP) Team visited NSGD Honolulu in August 1996. A primary purpose of the visit was to investigate the leakage of site-generated electromagnetic interference into the RF paths of the radio-frequency-distribution system (RFD). SNEP-team visits to other sites had revealed that site-generated EMI was sometimes present at the input terminals of receiving systems; however there is never sufficient time during a standard SNEP-team survey of a site to fully investigate the problem. Since external radio interference (usually power-line noise) was usually higher in magnitude than internally-generated EMI, a detailed investigation of the internal problem was delayed until a time and opportunity occurred to investigate the matter.

The external radio-interference problem at some receiving sites has now been reduced to manageable levels, and ongoing work on this problem is being pursued at other sites. A handbook[1] describing effective techniques to mitigate external radio interference from power lines has been completed. The procedures in this handbook, when strictly followed, significantly reduce the radio-interference level at the input to a site's receivers; in addition they often uncover lower levels of interference from internal sources of EMI. Internal EMI recently has been identified as the primary problem at some sites[2]. These findings place emphasis on an investigation of the extent of the internal EMI problem and on quantifying the leakage of EMI into the RF paths of the RFD. The CDAA site at NSGD Honolulu, Hawaii (located near the city of Wahiawa) was available for such a test. This particular site is supported by NRaD Activity Pacific, a key participant in SNEP team activities. Their personnel have a detailed knowledge of the site. Also, special instrumentation could be shipped to the NRaD Activity Pacific facility for storage and final tests prior to transportation to the CDAA site.

SNEP-team personnel participating in the test are listed in Appendix A.

---

1 Wilbur R. Vincent and George F. Munsch, *Signal-to-Noise-Enhancement Program Power-Line Noise Mitigation Handbook*, 3rd Edition, prepared for COMNAVSECGRU, N-44, March 1996.

2 GUA9609 SNEP Team, *RFI/EMI Survey, NSGA Guantanamo Bay*, Quick-Look Report, prepared for Commander, COMNAVSECGRU, N-44, September 1996.

2. BACKGROUND COMMENTS

Digital equipment and power-control systems have been introduced into receiving and data-processing sites with little regard for their potential impact on the primary mission of the sites. Many such systems inject significant levels of EMI current onto the grounds, cable shields, power conductors, conduits, air-conditioning ducts, pipes, and other conducting material in a site. This document explores the extent of the leakage of site-generated EMI into the RF paths. It also investigates the maximum tolerable levels of EMI current on a site's conductors from internal sources.

Figure 2-1 (910129 0929) shows an example of the harmful impact of site-generated EMI on the operation of a receiving system at a CDAA site. The EMI current flowing on the shield of the antenna cable to WARS is shown in the top amplitude-vs.-frequency view. A peak in the current (about 800 μA) was noted at 5.1 MHz. The middle amplitude-vs.-frequency view shows the EMI leakage into RFD Beam A-300. The leakage amplitude is about -105 dBm in a 300-Hz measurement bandwidth. This is about the average amplitude of SOI received by the antenna system. The time-history view shows the similar temporal structure of the EMI current and the EMI leakage into the RF path for Beam A-300.

The source of the EMI in Figure 2-1 was traced to a mid-sized computer located in another part of the facility. The shields of LAN cables, the shields of other conductors, and grounds running from this computer to other locations in the Operations building carried very high levels of EMI current. Direct-conducting, inductive-coupling, and capacitive-coupling paths spread the EMI onto other cables, throughout the site, and into the low-level RF paths.

Figure 2-2 (920812 1545) shows the impact of site-generated EMI on a small receiving site. The top amplitude-vs.-frequency view shows the ambient signals and the noise floor fed to a receiver over the frequency range of 15.5 to 31.5 MHz. Excessive noise was traced to a standard IBM-compatible desktop computer operating in the site. The middle amplitude-vs.-frequency view shows the ambient signals and the noise floor when the computer was turned off. The time-history view shows the change in the noise floor when the computer was turned off. A distinct reduction in the EMI level fed to a receiver is shown in this view.

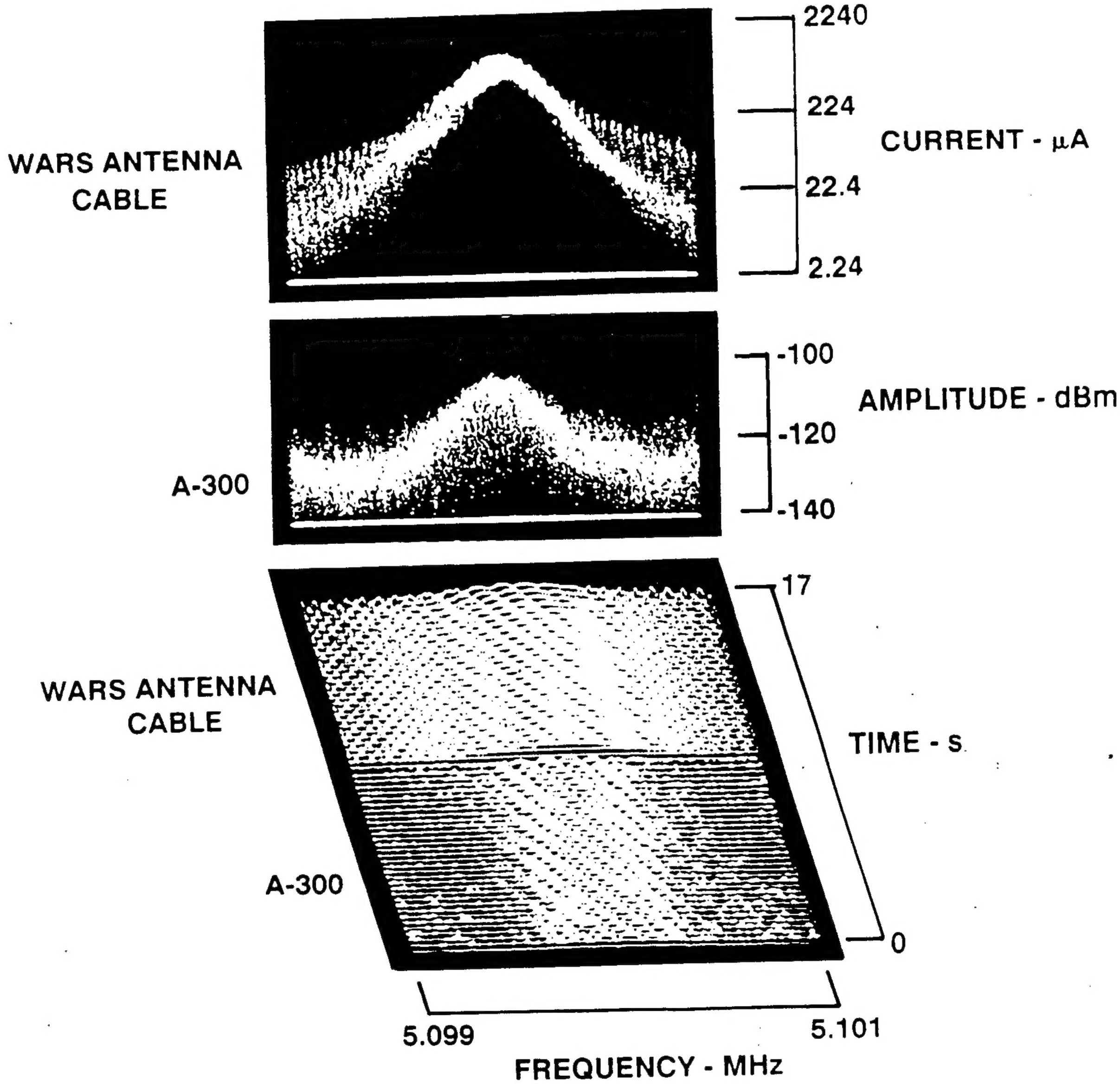

910129 0929
WAH; Bottom, A-300
Top, Probe on WARS Cable, W. Wall
5.1 MHz, 2 kHz, 0.3 kHz, 200 ms
Bottom: BPF #1, +20, PS, 0, -40
Top: F-70, BPF #1, +20, PS, 0, -40

Figure 2-1
Example of the Adverse Impact of Site-Generated EMI on Signal Reception at a Large Site

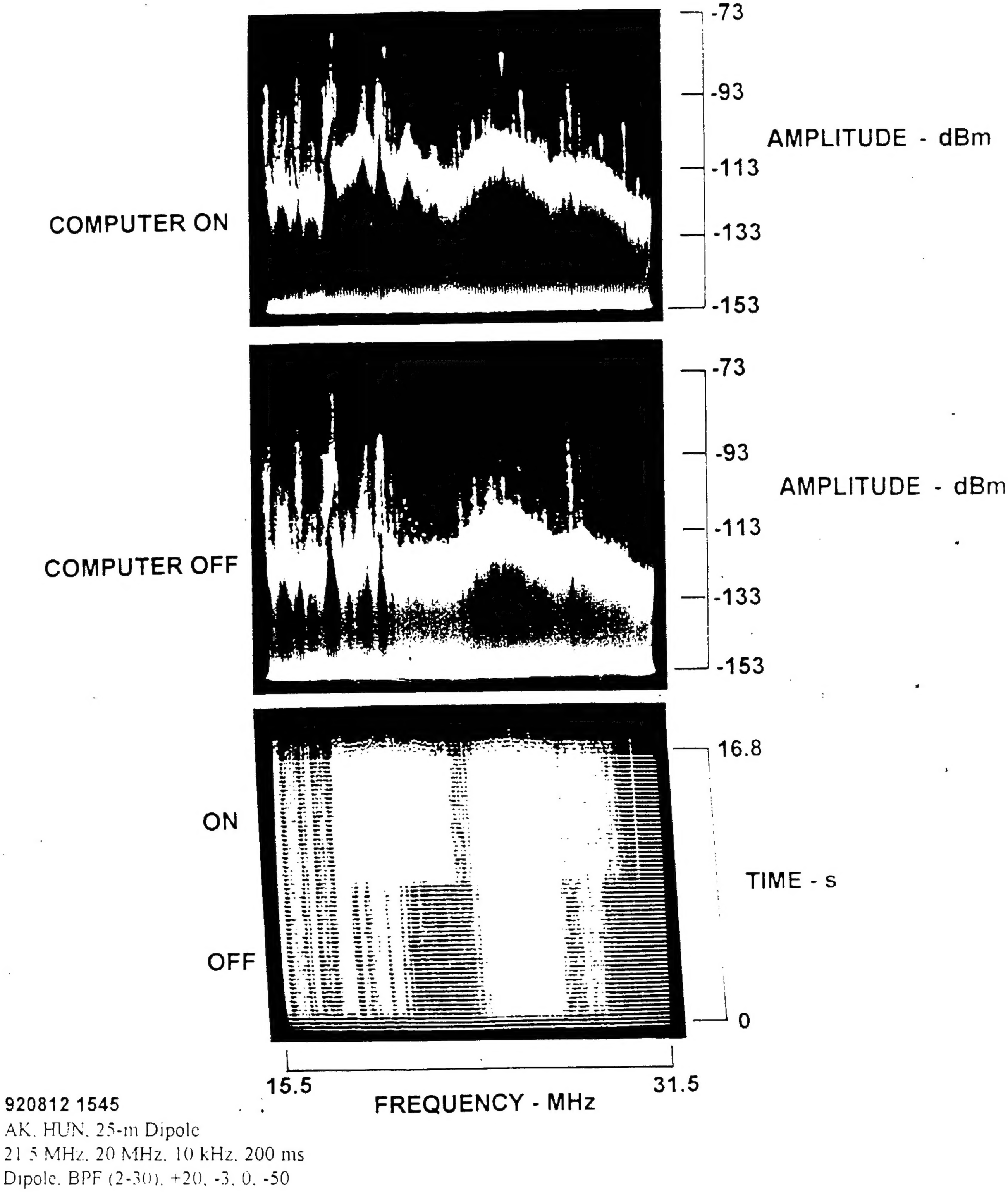

Figure 2-2
Example of the Adverse Impact of Site-Generated EMI on Signal Reception at a Small Site

The source of the computer-generated EMI in Figure 2-2 was traced to radiation from a modem cable running from the computer to a telephone jack. When this cable was disconnected from the computer, site-generated EMI was not detectable at the receiver input. Direct radiation from the computer did not affect the noise floor or the operation of the site.

A third example is provided to show that the internal EMI problem also extends upward into the VHF and UHF bands. Figure 2-3 (960924 0945) shows EMI at the input terminals of a receiver in the upper part of the VHF band. Bands of EMI are spaced about 1.6-MHz apart across the entire width of the frequency range examined. Excessive levels of EMI were found from the lower end of the HF band upward into the UHF band. The source was traced to the synchronizer unit of the site's video security system (VSS).

One aspect of the VSS example should be noted. Due to the high signal environment, a preamplifier could not be used to lower the noise figure of the measurement system to that of the receiving system. The noise floor of Figure 2-3 is more than 20-dB higher than the receiving system. Thus the impact of the EMI on the receiving system is much greater than implied by a casual glance at the measured data.

The three examples showing the impact of internally-generated EMI on the reception of radio signals are typical of numerous other examples obtained at both small and large receiving sites. While a collection of such examples has accumulated over several years of measurements at receiving sites, a comprehensive examination of the overall problem was not made until the tests at NSGD Honolulu. External EMI from sources on power lines was an even larger problem, and most of the SNEP-team resources were directed at the larger problem. Nevertheless, the presence of many examples of the detrimental impact of internal EMI on signal reception lying in the files reminded team members that this next-larger problem needed attention. The injection tests at Wahiawa described in this document constitute the beginning of the investigation of this larger problem and the start of developing effective mitigation actions. This document is a partial record of the results of the Wahiawa injection measurements.

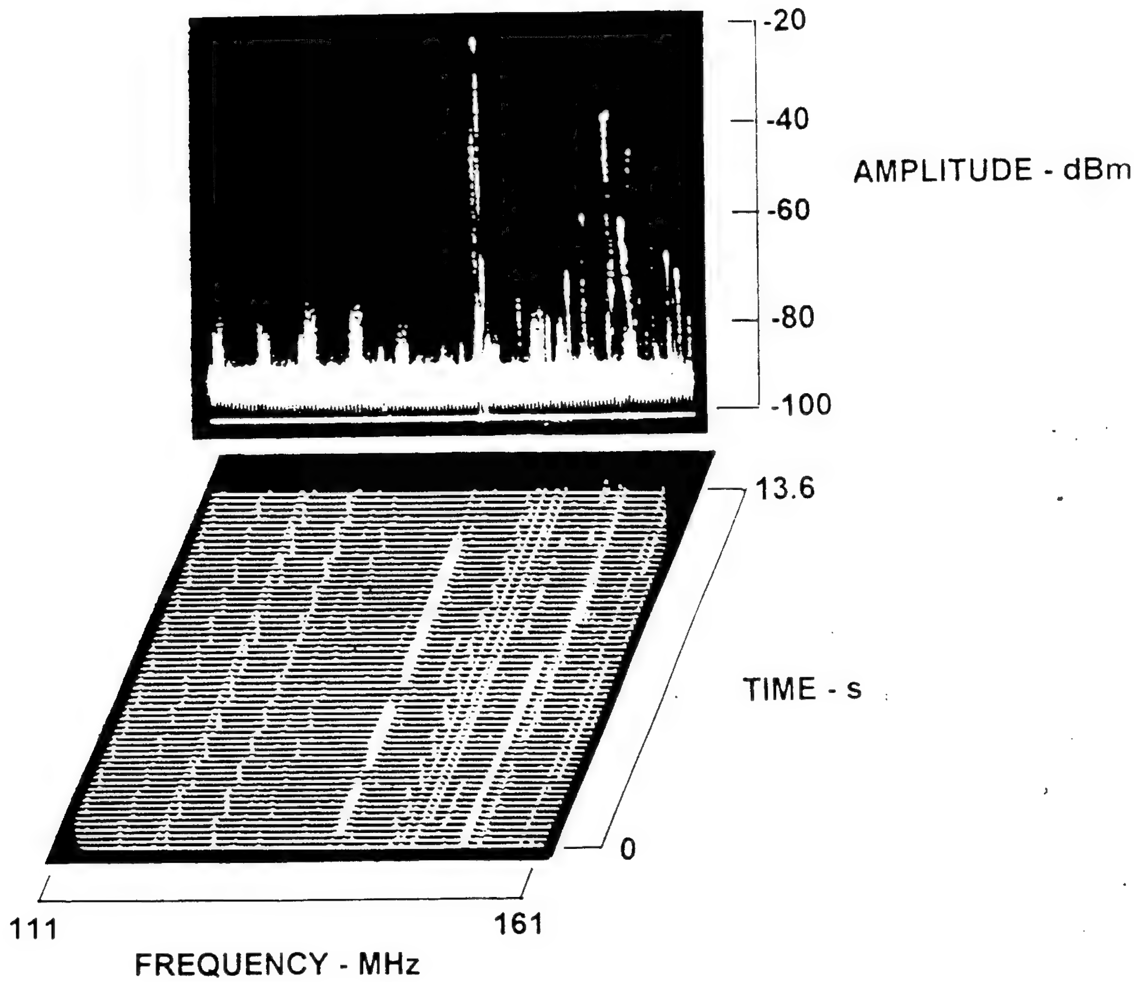

960924 0945
GTMO. OPS. LPA3-V
136 MHz, 50 MHz, 30 kHz, 200 ms
0, 0, -20
Vss Interference
4.71 to 4.77 MHz basic sweep frequency

Figure 2-3
Example of the Adverse Impact of Site-Generated EMI on Signal Reception at a VHF/UHF Site

3. IMPLEMENTATION

3.1 Instrumentation

The instrumentation required to inject known levels of current into grounds, cable shields, conduits and other conductors was assembled and tested at the Naval Postgraduate School. It was then packed and shipped to NRaD Activity Pacific. The new facility of NRaD Pacific was efficiently designed for the convenient receipt and storage of instrumentation and for the checkout of equipment. NRaD also provided additional instrumentation and personnel to aid in the conduct of the tests. An NRaD van was used to transport the instrumentation to the NSGD Honolulu site.

Figure 3.1-1 is a block diagram of the injection equipment.

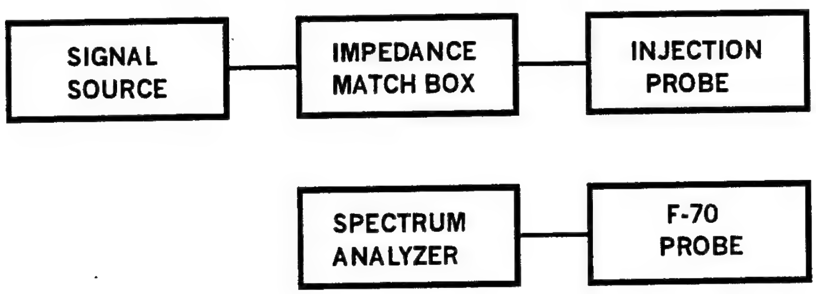

Figure 3.1-1
Injection Instrumentation

The upper row of Figure 3.1-1 shows the injection instrumentation. The signal source was a Kenwood Model TS-50 Transceiver which had been modified to generate a signal at any desired frequency between 2 and 30 MHz. Power output could be varied from very low levels up to a maximum of 100 watts for short periods of time. Several models of impedance match boxes were used to match the 50-ohm output of the TS-50 unit to the injection probe. Standard amateur radio match boxes were used. Since the driving impedance of the injection conductor was reflected back into the signal source, it was necessary to cope with a wide range of driving impedance values. The injection probe contained taps on its winding to aid in impedance matching. It was a custom made probe designed for the injection of HF current into conductors.

The second row of instrumentation in Figure 3.1-1 provided a means to measure the level of the injection current. A Fischer Model F-70 Current Probe was used as a current sensor and a standard spectrum analyzer was used to measure the amplitude of the current. The TS-50 power output and the match box were adjusted to obtain a desired level of injection current.

Figure 3.1-2 shows the instrumentation used to measure the amplitude of the test signal appearing at an output port of the RFD. The RFD output port for the test receiver located in the RF Room was used. The amplitude at the input of the site receivers would be about 1 or 2 dB less than the recorded data because of the added attenuation of the cable running from the output port of the RFD. This loss was ignored for the purposes of this measurement.

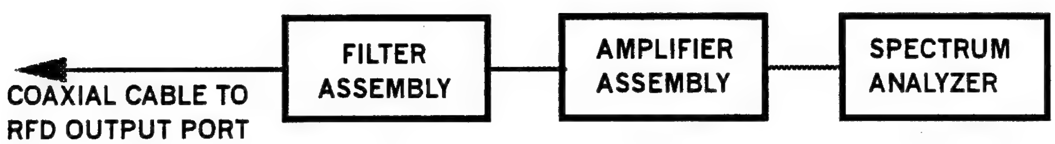

Figure 3.1-2
Signal Leakage Measurement Instrumentation

The signal measurement instrumentation was very simple. It consisted of set of bandpass filters to limit the total signal power into the instrumentation, a preamplifier assembly with a gain of 20 dB, and a spectrum analyzer for signal-level measurements. A standard SNEP preamplifier assembly was used to obtain a signal-measurement sensitivity near that of a standard HF receiver. The goal was to be able to detect a signal level as low as -130 dBm in a 3-kHz gaussian-shaped bandwidth. Hewlett Packard Series HP-141 and Model 8560 Spectrum Analyzers were used to measure leakage signal levels. Both models of analyzers provided consistent, reliable, and repeatable amplitude measurements.

The instrumentation permitted the measurement of leakage signals along with ambient signals and noise from the antenna. The test frequency was varied up or down a few kilohertz to avoid strong signals. Alternatively, the input to the primary multicouplers could be terminated to remove ambient signals and external noise. Most measurements were made with the antenna connected in order to provide realistic information involving all possible RFD leakage mechanisms.

3.2 EMI Leakage, Initial Test

An initial test of leakage was made prior to starting the measurements for a series identified as Tests 1 through 5. The initial test was made to check the operation of the injection and measurement instrumentation, and to become acquainted with the extent, if any, of leakage from the test point into the RF paths. The results of the complete test series are described later in this section. For this initial test a discrete-frequency EMI signal was injected onto the shield of the coaxial cable running from the ground floor RF Room to the WARS located in an operational area on the second floor. The test configuration is described more completely in Section 3.3 (see Test 1).

Figure 3.2-1 shows the results of the initial test at a frequency of 2.1 MHz.

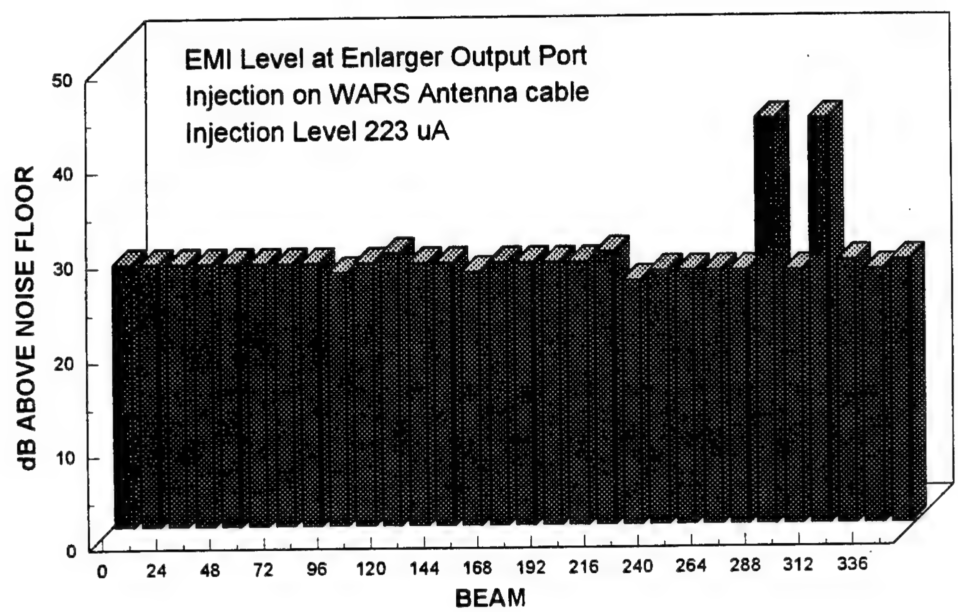

Figure 3.2-1
EMI Leakage from Initial Test

Leakage into the RF path provided for the test receiver in the RF Room is shown. The amplitude of the leakage signal is provided in dB above the receiver noise floor when the noise floor is measured in a 3-kHz gaussian shaped bandwidth. The actual leakage level can be reconverted into dBm by subtracting 130 from each value shown in the figure.

One primary aspect of the data is evident from a cursory examination of the example. Excessive test-signal leakage was found for Beams LBM-288 and LBM-312. Leakage for these two beams was 15-dB higher than that of all other beams. This leakage was quickly traced by NRaD personnel to faulty coaxial connectors in RF paths for the two beams. The connectors were repaired before starting the sequence of measurements described in Sections 3.3 through 3.7. The example is shown to demonstrate the destructive impact on signal reception from improperly assembled and defective coaxial cables and connectors in the RFD. EMI current will efficiently seek such weak spots in the RFD and appear as harmful and destructive interference at the input terminals of a receiver.

A second factor of high interest is also shown in Figure 3.2-1. The injection current of 707 μA (a value of EMI current often found on the WARS RF cable at CDAA sites) produces interference levels about 30-dB above the noise floor in the RF path feeding the test receiver in the RF Room. This is a very high level of interference. It indicates that the RF paths are poorly isolated from site-generated EMI current flowing on the WARS antenna cable and probably from site-generated EMI current flowing on other conductors.

One can assume that if the EMI current is reduced in level by 30 dB, the interference level should be reduced to the noise floor. This suggests that the maximum EMI current that can be tolerated is about 22.4 μA. This is much lower than the EMI current levels found on the WARS antenna cable in most sites and lower than the EMI current levels found on many other conductors in a receiving site.

This initial measurement provided useful guidance for the conduct of the more comprehensive test series.

The implications of the leakage results are more completely discussed in Section 4.

3.3 EMI Leakage, Test 1

Figure 3.3-1 provides a sketch of the layout of Test 1. EMI current at a preset level was injected onto the shield of the double-shielded coaxial cable leading from the RF Room to WARS. The WARS system was provided with signals from a distribution plate inside Bay 4 of the RF Room rather than from an output port of ENLARGER. EMI leakage into the RFD was then examined at the output port of ENLARGER serving the test receiver position in the RF Room. A Fischer Model F-70 probe and a spectrum analyzer were used to set the injection current to a prescribed level.

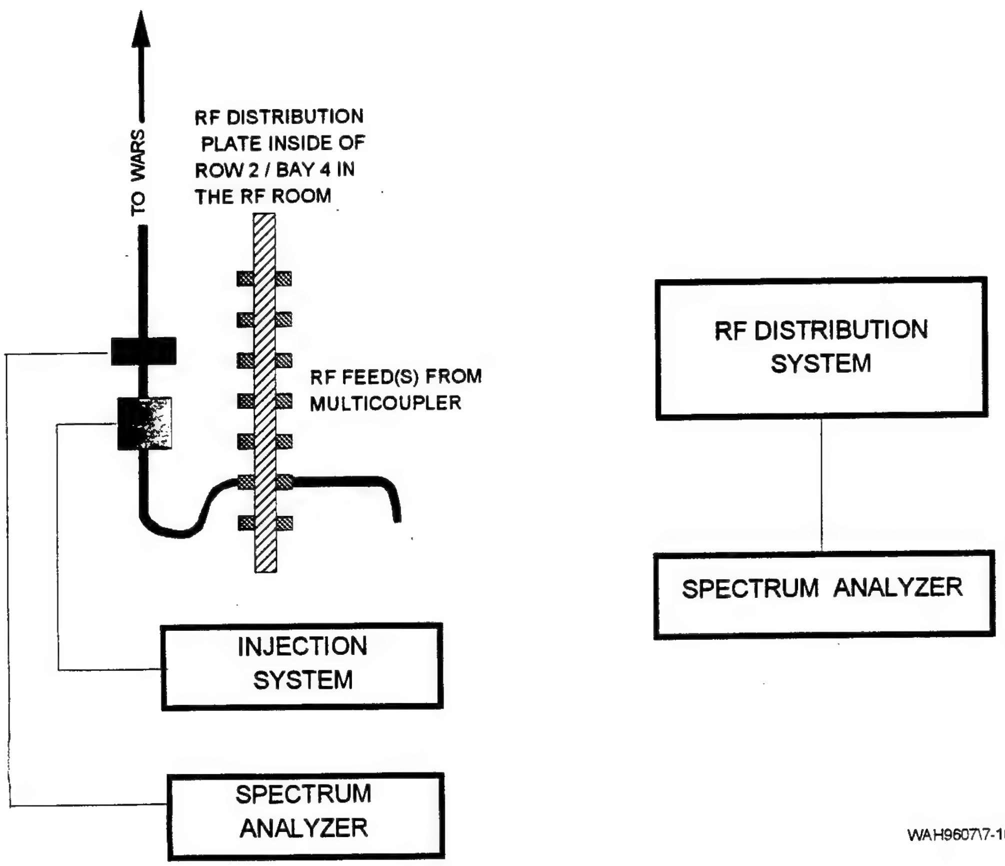

Figure 3.3-1
Block Diagram for Test 1

The test signal was set on a preset frequency and amplitude, the spectrum analyzer was tuned to the test frequency, and the ENLARGER azimuth control was sequentially stepped through all beams. The leakage signal level was measured for all beams. This process was

repeated at 1-MHz intervals over the frequency range of 2 to 30 MHz. For this test, the injection current was adjusted to 707 μA, an EMI level often found on RF cable shields in CDAA sites.

Figure 3.3-2 shows the leakage signal for six frequencies in the low-band. Signal amplitude is shown on the Y-axis, beam heading on the X-axis, and frequency on the Z-axis. The leakage values are expressed in dB above the RFD noise floor of -130 dBm (the approximate noise floor of a primary multicoupler for a 3-kHz gaussian-shaped bandwidth). Note that Beams 288 and 312 have somewhat higher leakage than most other beams. The EMI leakage varied from about 20- to a peak value of 69-dB above the noise floor, implying a maximum tolerable EMI level of 0.25 μA.

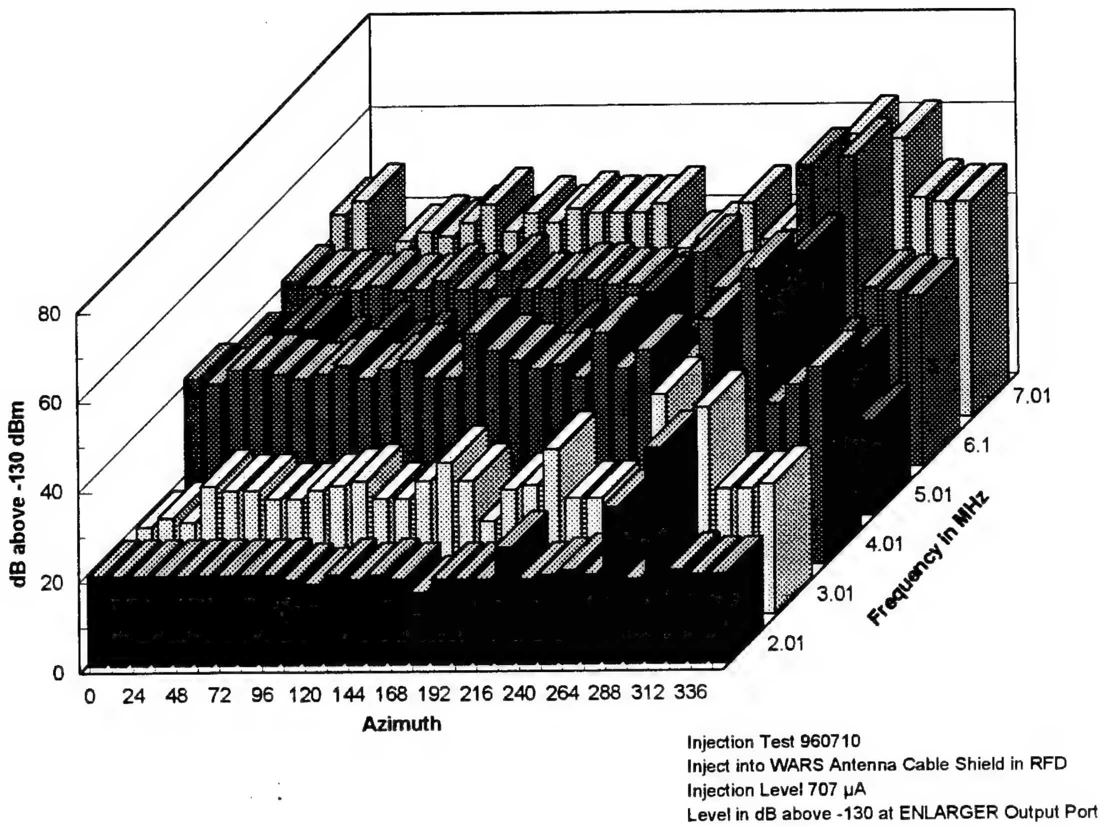

Figure 3.3-2
Low-Band EMI Leakage, Test 1

Figure 3.3-3 shows leakage into the RFD from EMI current flowing on the shield of the WARS coaxial cable for 20 frequencies in the high band. Leakage is shown for each test frequency and for all CDAA beams. The high-band leakage was considerably more uniform

than for the low-band. No major resonance effects were noted. The leakage signal varied from 40- to a peak of 68-dB above the noise floor. The maximum EMI leakage current that can be tolerated on the shield of the WARS antenna cable without interference to low-level signals of interest (SOI) would be 68-dB below the injection current. This yields a maximum tolerable value of EMI shield current of 0.3 μA for a 0-dB (S+N)/N EMI detection level.

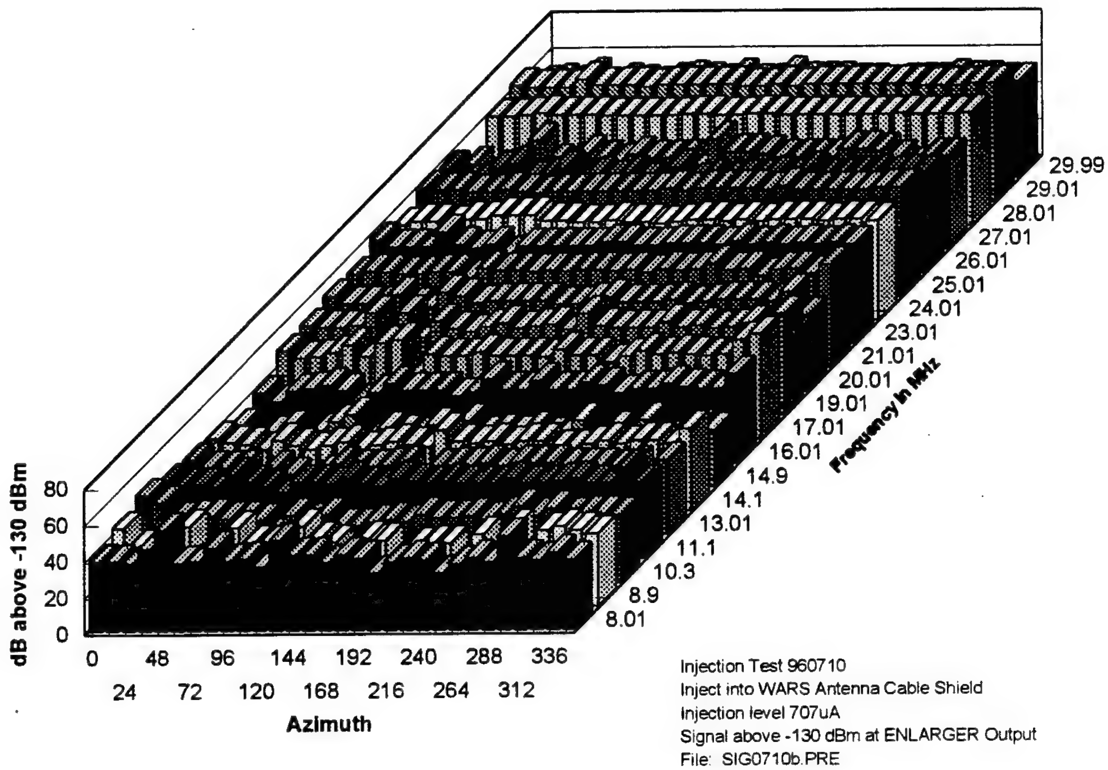

Figure 3.3-3
High-Band EMI Leakage, Test 1

The maximum tolerable injection current is somewhat less than the previously suggested maximum level[3] of 2 μA for EMI current on cable shields, grounds, and other conductors. It is also considerably lower than EMI current levels commonly found in receiving sites. Even greater protection would be required for the detection of spread-spectrum signals received at amplitudes below a 0-dB (S+N)/N threshold level.

---

[3] Wilbur R. Vincent and Richard W. Adler, *The Control of Intra-Site Sources of RFI/EMI at Naval Receiving Sites*, Technical Memorandum WV940411, November 1994.

3.4 EMI Leakage Test 2

Figure 3.4-1 shows the measurement configuration for Test 2. The instrumentation was similar to that in the previous test, but the injection probe was moved to the ground bus running under the ENLARGER bays. The ENLARGER bays and other RFD system components were grounded to this bus. The bus was electrically connected to other building ground buses and eventually to an earth ground located several hundred feet from the injection location.

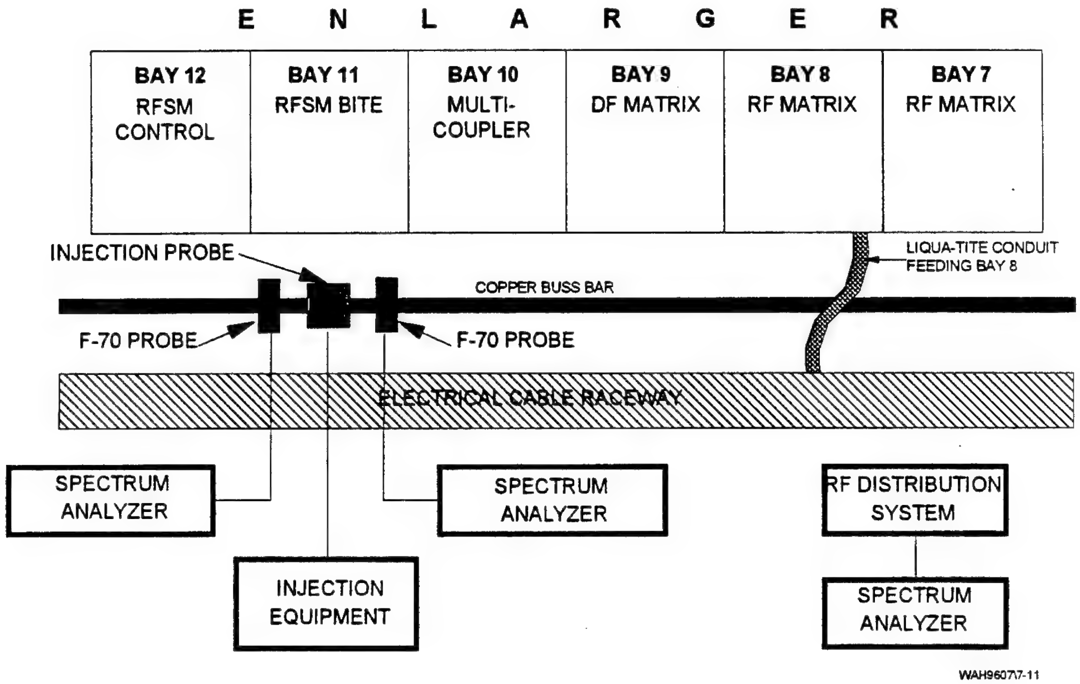

Figure 3.4-1
Block Diagram for Test 2

The injection and measurement process for Test 2 was identical to that for Test 1. The injection level, 707 μA, was the same as for Test 1.

Figure 3.4-2 shows the EMI leakage levels for beams in the low band. Seven test frequencies spaced 1-MHz apart were used. The result at 8.01 MHz is repeated in the high-band data. The amplitude scale was made equal to that of the prior example.

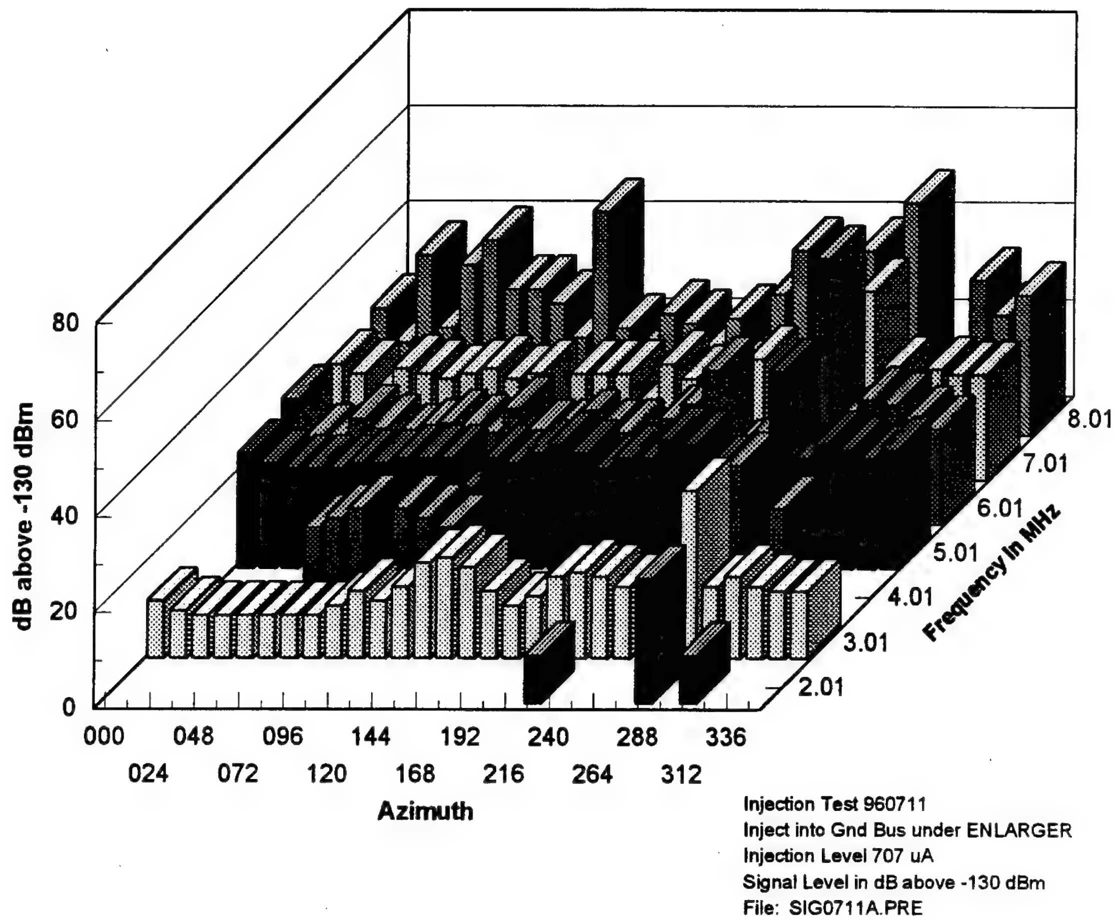

Figure 3.4-2
Low-Band EMI Leakage, Test 2

EMI leakage could be measured on only three low-band beams at 2.01 MHz and only eight beams at 4.01 MHz. Leakage was somewhat easier to measure at the higher frequencies. Large variations in leakage signal level were found, indicating that the leakage paths contained large resonances. This is a reasonable conclusion since sections of ground bus lengths and other conductor lengths were at resonant lengths for the higher frequencies. The maximum leakage level at the low-band was 55-dB above the system noise floor. This suggests that the maximum tolerable EMI current on the ground bus (for a 0-dB (S+N)/N ratio) would be about 1.3 μA for the low-band frequencies.

The comparable high-band leakage is shown in Figure 3.4-3.

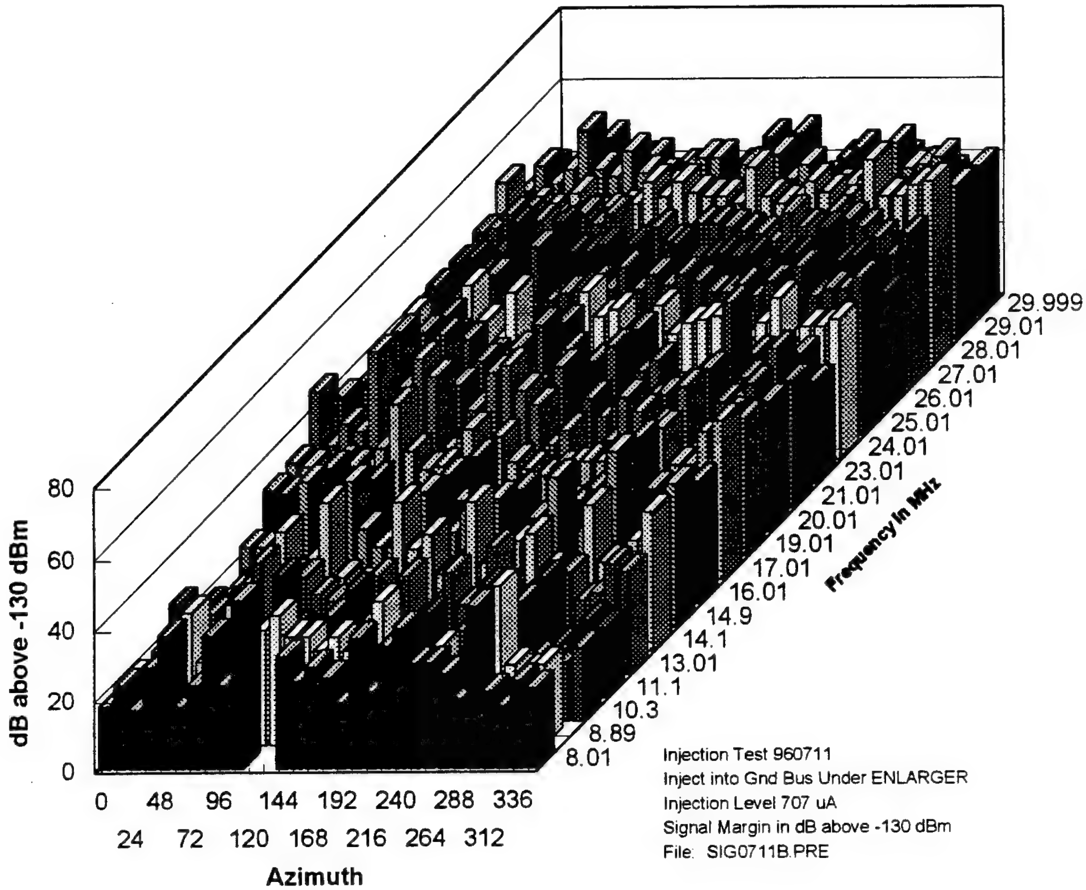

Figure 3.4-3
High-Band EMI Leakage, Test 2

The maximum high band leakage was 59 dBm. This indicates that the EMI current must be reduced to 0.8 μA to be at the noise level of the primary multicouplers for a 3-kHz detection bandwidth.

3.5 EMI Leakage, Test 3

Figure 3.5-1 shows a sketch of the measurement configuration for Test 3. The test signal was injected into one of the RG-85 cables leading from the RF Room to the antenna elements. The injection probe was located outside the RG-85 cable termination plate.

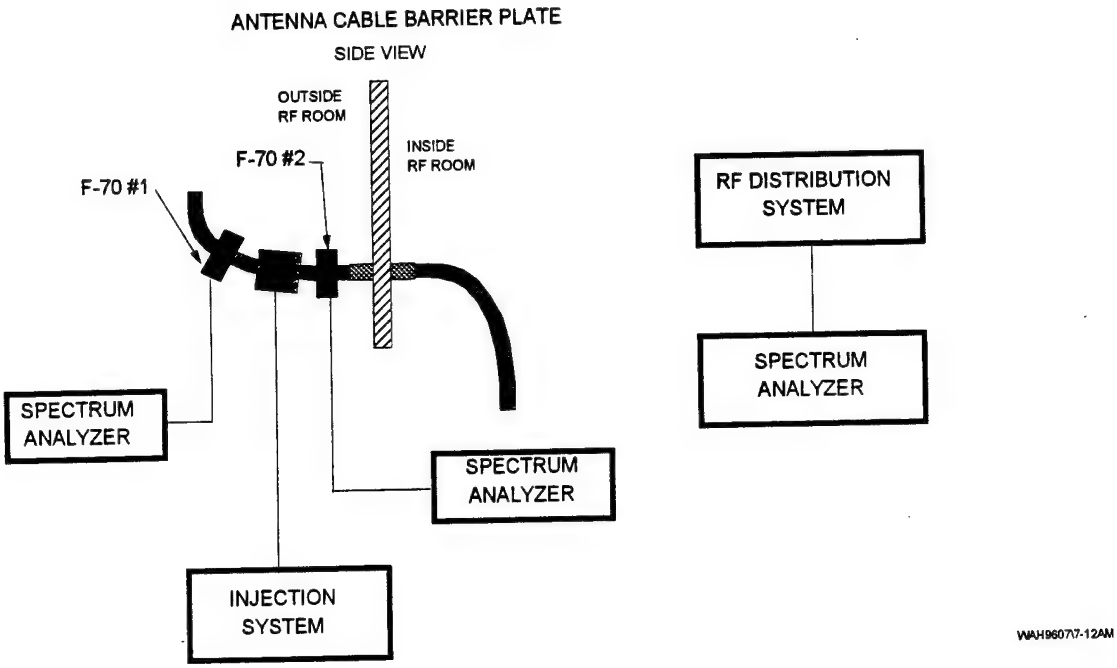

Figure 3.5-1
Block Diagram for Test 3

The low-band injection was increased to 7070 μA to produce a useful leakage value for a reasonable number of the beams. The low-band results for Test 3 are shown in Figure 3.5-2.

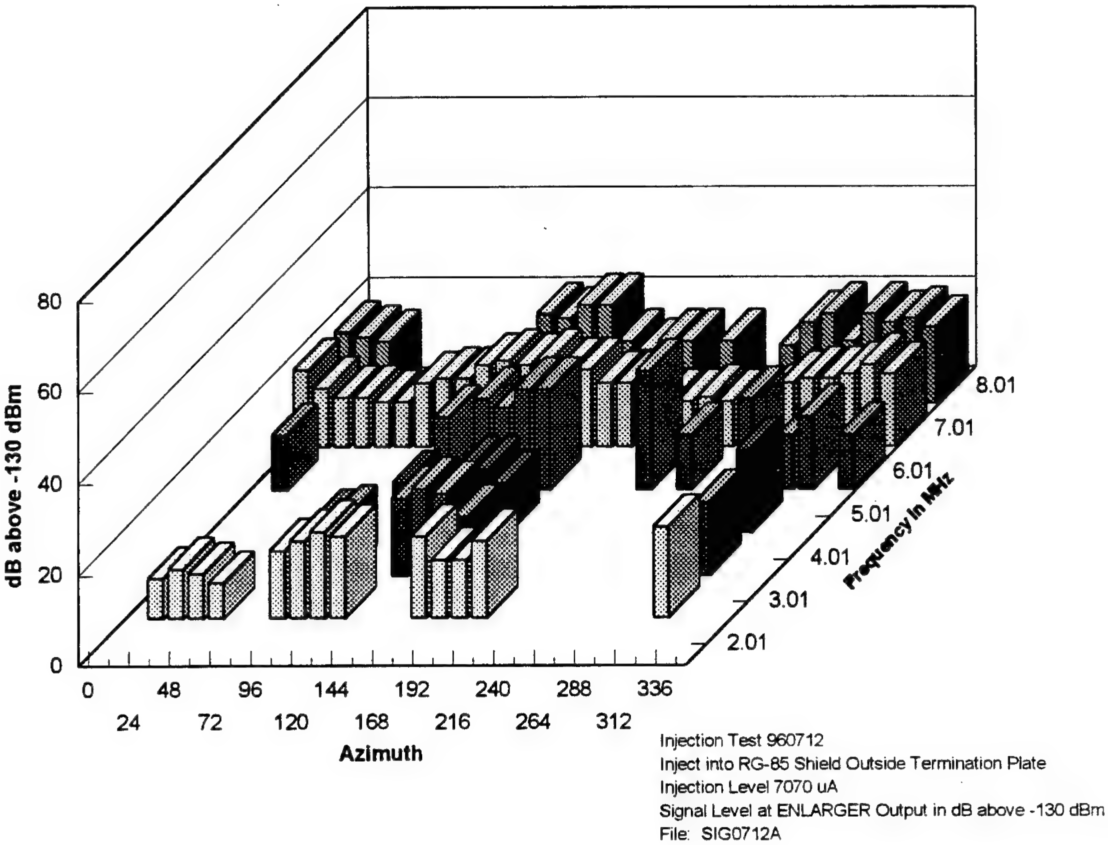

Figure 3.5-2
Low-Band EMI Leakage, Test 3

Data could not be obtained for about half the beam-frequency cases due to resonance effects in the cables, ground conductors, and the leakage paths. The maximum leakage level was 26-dB above the noise floor, indicating that EMI currents up to about 362 μA could be tolerated on the RG-85 antenna cable shield. The higher tolerable level of EMI current on the shield of the RG-85 cable suggests that some EMI isolation to internal RFD leakage paths is provided by the antenna cable termination plate. This was one of the original purposes of the termination plate, and it appears to have retained some of its isolation capability even though the plate is now located inside the expanded building.

Figure 3.5-3 shows the high-band results for Test 3

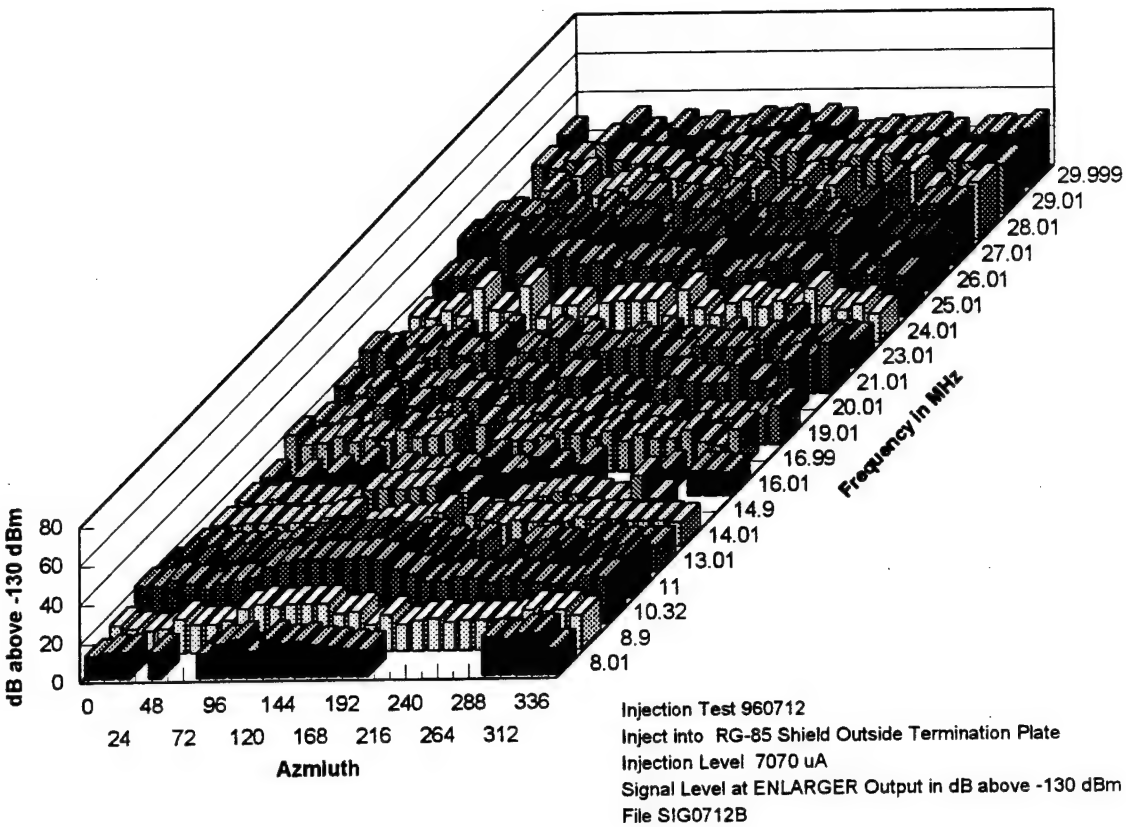

Figure 3.5-3
High-Band EMI Leakage, Test 3

While more data slots were filled for high-band Test 3, the end result was about the same as for the low-band. The maximum leakage level was 43-dB above the noise floor. This indicates that EMI current levels of 50.1 μA can be tolerated on the shield of this cable over the total frequency range of the high band. This indicates that the RG-85 antenna coaxial cable was reasonably well isolated from leakage paths in the RFD.

3.6 EMI Leakage, Test 4

For Test 4 the injection probe was moved to the shield of the RF cable for antenna element LB-16 located inside the antenna cable barrier plate. Figure 3.6-1 shows the test configuration. The injection level remained at 7070 μA.

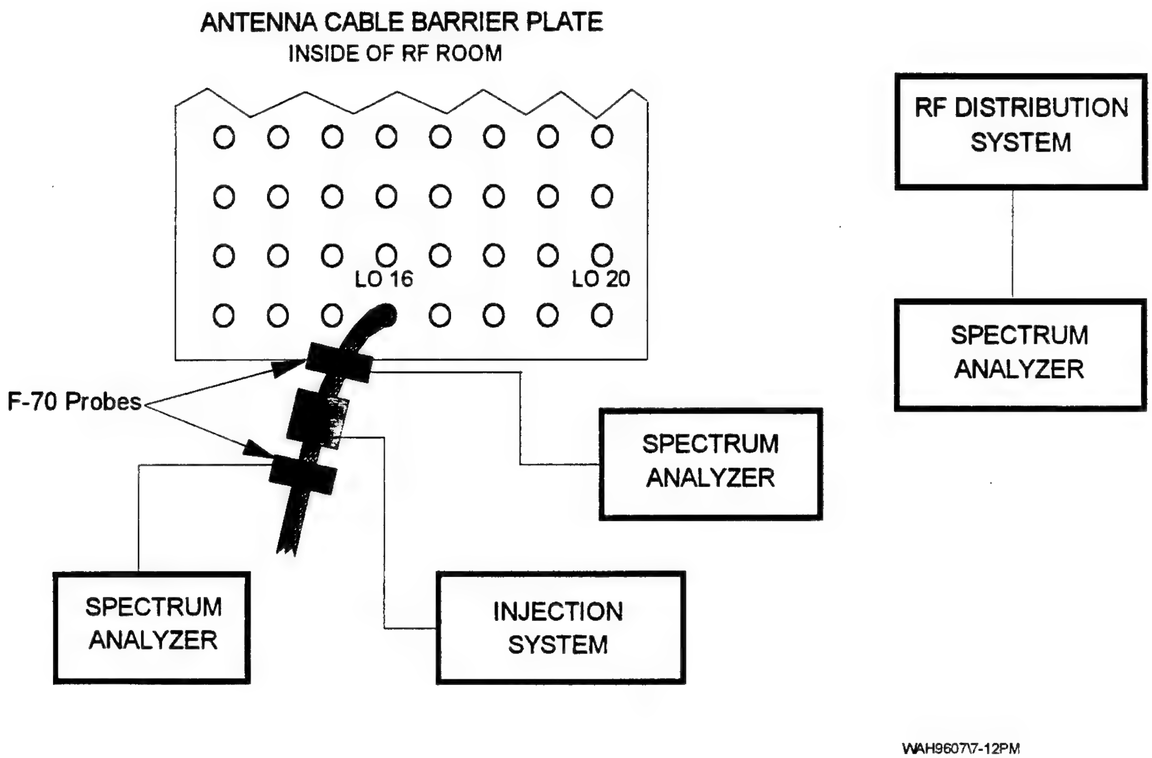

Figure 3.6-1
Block Diagram for Test 4

Figure 3.6-2 shows the result of the low-band measurements. Data were obtained on most of the beam-frequency slots. Of interest is that six beams from 108° to 168° appear to have less EMI isolation than the remaining beams. The maximum level of EMI coupled into the RFD occurred for these beams, and it was 44-dB above the noise floor. This indicates that a maximum level of EMI current of about 44.6 μA can be tolerated for a 0-dB (S+N)/N detection level at the low-band frequencies.

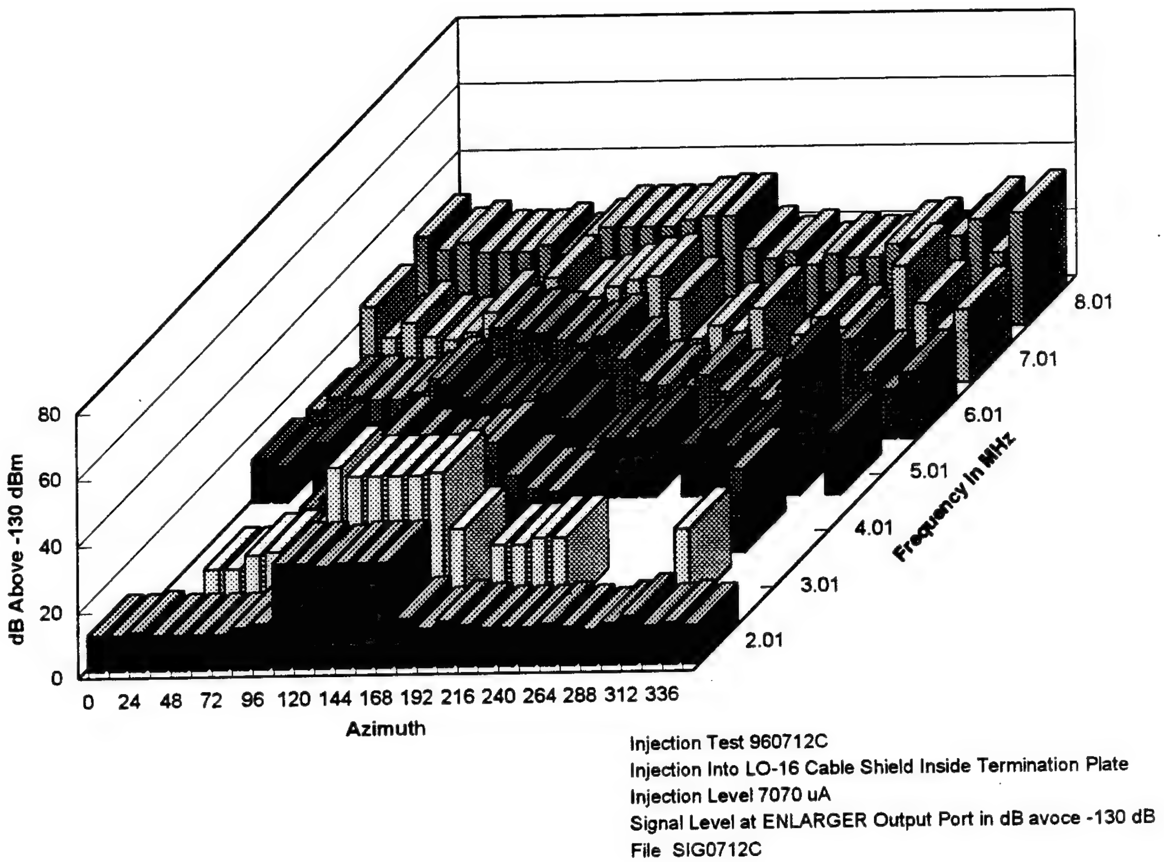

Figure 3.6-2
Low-Band EMI Leakage, Test 4

Figure 3.6-3 shows the high-band data for Test 4. The injection current level remained at 7070 μA for the high-band measurements.

The high-band data show a maximum EMI leakage level 38-dB above the noise floor. This indicates that the maximum EMI current allowable on the shield of the coaxial cable running from the termination plate to the primary multicouplers is 89 μA. The high-band isolation is somewhat lower than for the low-band.

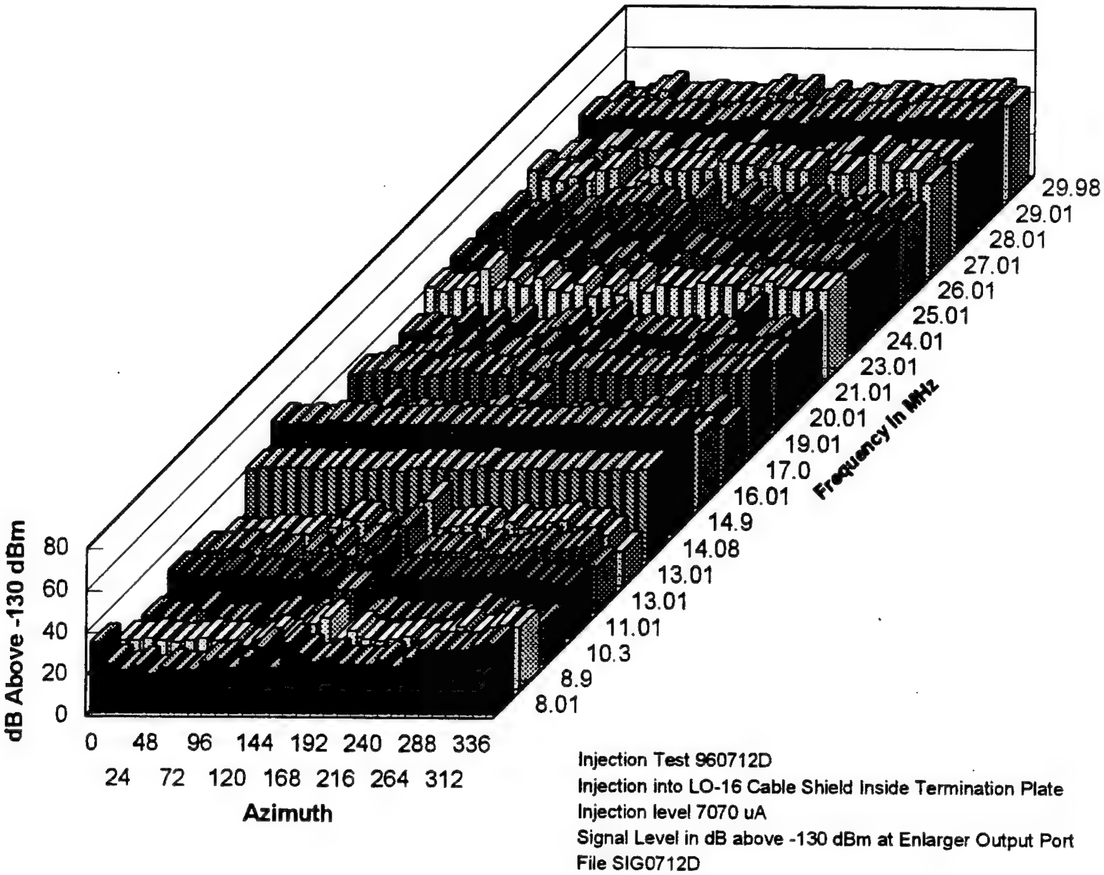

High-Band EMI Leakage, Test 4

The data from the low-band and high-band tests suggest that the cable from the termination plate to the primary multicouplers is reasonably well isolated from the RFD output ports. This suggests that the primary leakage into the RFD does not take place at or near the input to the primary multicouplers. When compared with the results from Test 3 (Injection outside the termination plate) the data suggests that the termination plate in its present configuration provides about 15-dB of electromagnetic isolation from the RF Room at the low band and slightly more for the high band. It is estimated that the original building configuration, where the termination plates were located on the outside walls of the building, would provide 30 to 40 dB of EMI isolation.

3.7 EMI Leakage Test 5

Test 5 investigates EMI coupling between the green-wire ground conductor located in Power Panel TP-003-1 and the RFD output port. Power is provided to equipment in the RF Room by this panel. All green wires from equipment served by this panel are joined together in the power panel. The injection was made at the single green-wire conductor running from the panel to the building neutral-ground bond. Figure 3.7-1 shows the test configuration. The injection current was reduced to 707 μA for this test.

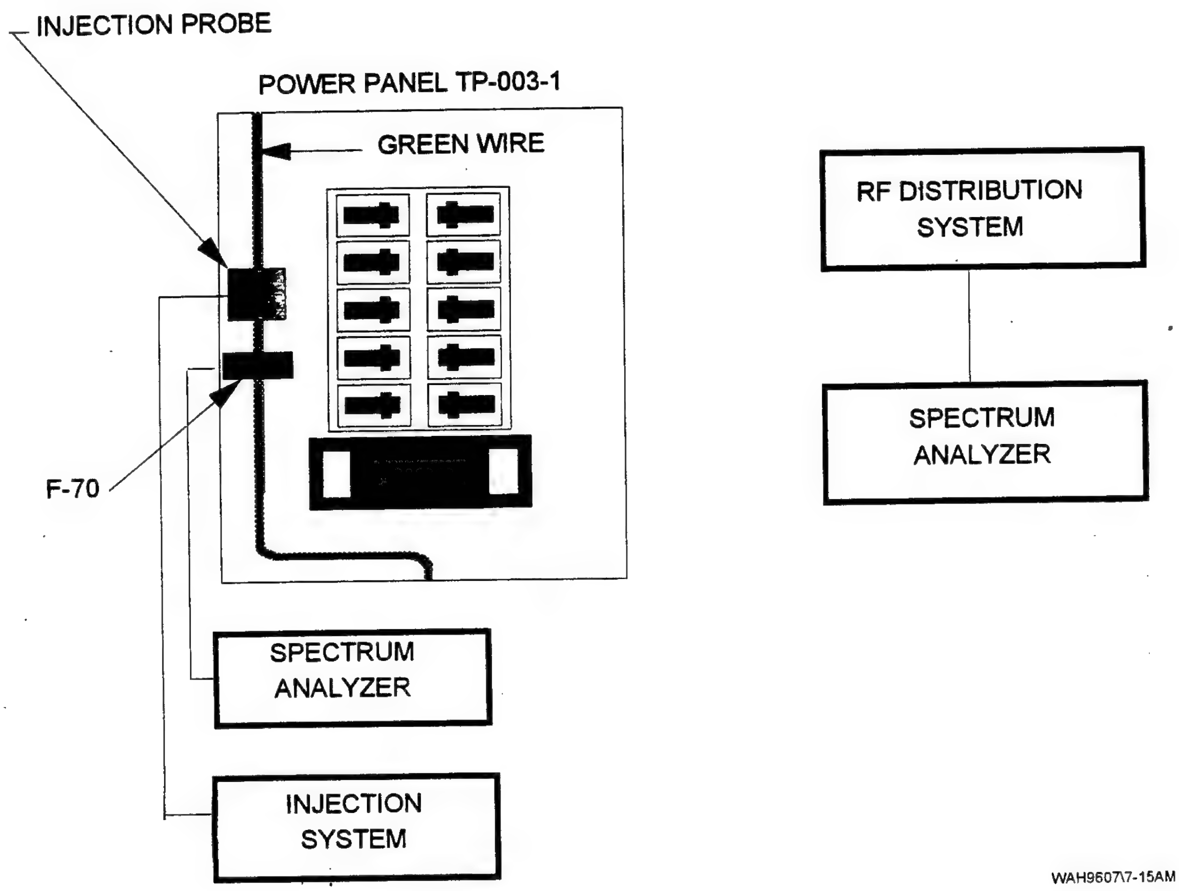

Figure 3.7-1
Block Diagram for Test 5

Figure 3.7-2 shows the EMI leakage from the green-wire ground conductor into the RFD for the low band.

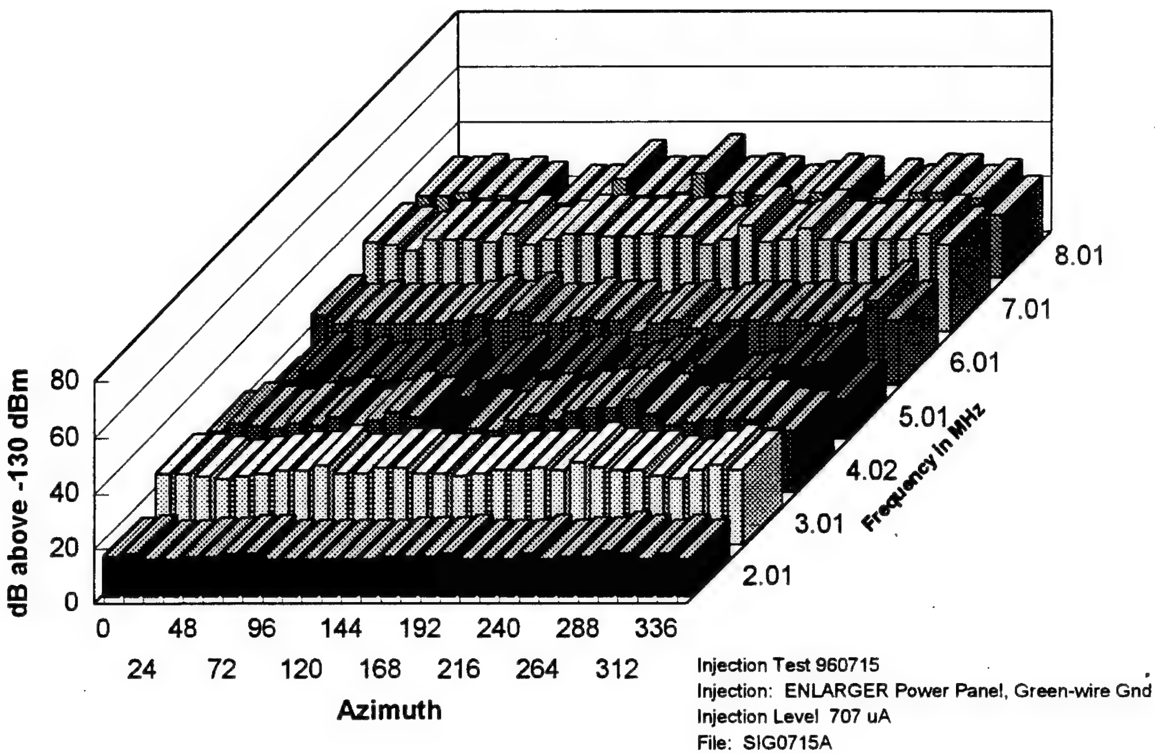

Figure 3.7-2
Low-Band EMI Leakage, Test 5

The maximum low-band leakage was 38-dB above the noise floor. The leakage was fairly uniform from beam to beam on many of the test frequencies. A few significant variations in leakage were found at some test frequencies, indicating the presence of a few resonance conditions. The data suggests the maximum tolerable EMI current in the green-wire power conductor is about 8.9 μA for the low-band beams.

The companion high-band data for Test 5 is shown in Figure 3.7-3.

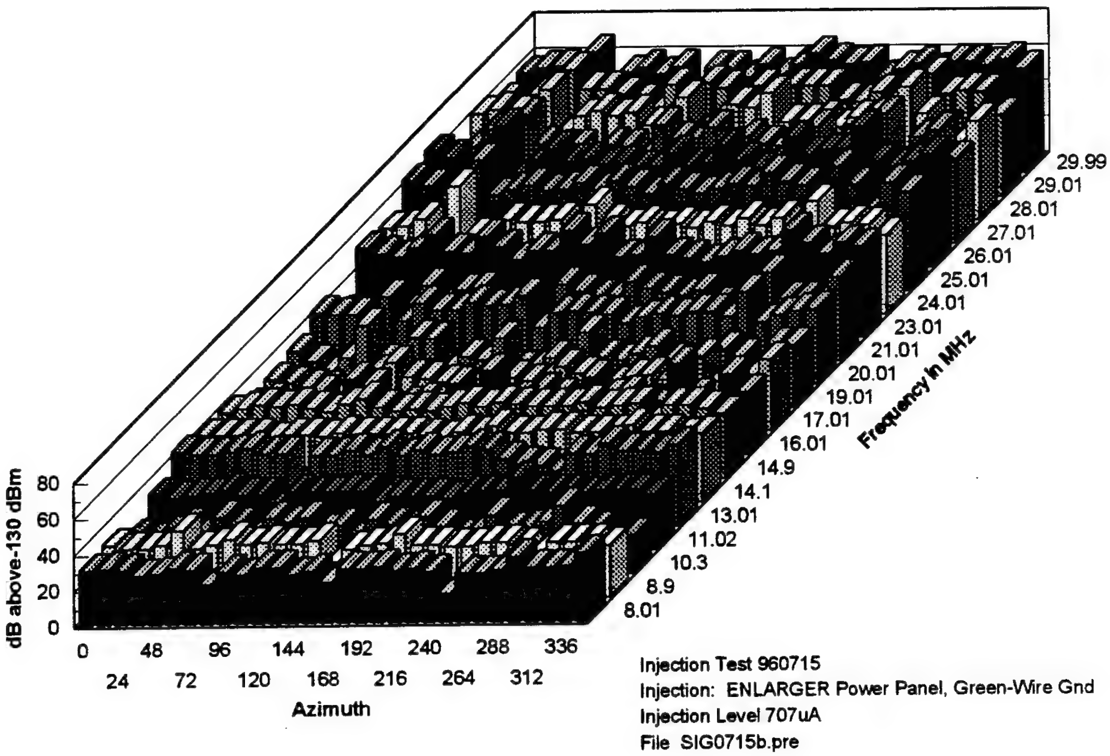

Figure 3.7-3
High-Band EMI Leakage, Test 5

The maximum high-band leakage from the green-wire conductor in the power panel varied from about 20-dB to as high as 60-dB above the RFD noise floor. This suggests that the maximum tolerable EMI current for the high band is about 0.7 μA. It is curious that the leakage from the green wire into the RFD is greater for the high band than for the low band. This is the opposite of the prior example. However, this finding is consistent with prior observations of high levels of the ENLARGER Beam-Path Verification signal (near 32 MHz) on conductors in its power panel. These two results suggest that some aspect of the high-band signal paths of the RFD lack electromagnetic isolation from the power conductors. These findings also suggest that the EMI leakage mechanism between the RFD and the power conductors is different from those associated with coaxial cable shields and grounds. It further demonstrates the need for the complete shielding and isolation of all RF paths.

4. DISCUSSION

4.1 General Comments

The EMI leakage tests described in previous sections were made at a typical CDAA site, NSGA Wahiawa. The site is considered by the team to be in good physical and electrical condition from the standpoint of today's installation, maintenance, and operational practices and procedures. The CDAA structure is a standard AN/FRD-10. The Operations Building is a durable concrete structure commonly employed in such sites. The equipment in the RFD portion of the site is considered to be in accordance with normal site complements. A standard ENLARGER RF switch was installed at the site for the selection of beams. All single-shielded coaxial cable installed in the RFD during the ENLARGER installation had been replaced with double-shielded coaxial cable. No attempt was made to alter or change the state of the site's RFD or other system for these measurements.

Section 2 describes a few typical cases of the impact of EMI current on the reception of radio signals at other receiving sites. Similar examples have been found at almost all receiving sites visited by the authors (a total of 41 different sites). All available information suggests that a common EMI problem exists in most, if not all, of our HF, VHF, and UHF receiving sites. The examples show that changes in site design, installation practices, and maintenance practices are required to avoid EMI leakage into the low-level RF paths of existing and new sites. Effective mitigation actions must be defined for existing HF, VHF, and UHF receiving sites if they are to effectively accomplish their primary mission, the reception and detection of SOI.

When considering the leakage tests described in Section 3, it must be remembered that many very strong signals of little or no interest are intercepted by our receiving sites. The often quoted saying *"we are already receiving far too many signals and thus can afford to lose a few"* is partly true, but it must be placed in proper context. The total number of signals received at any intercept site includes a massive number of strong signals that are of absolutely no interest. There is no practical way of limiting the number of the strong signals except by the use of filters, but filters limit the frequency coverage of the sites. Most of the signals of high interest are very low in amplitude, and they must be sorted from the much larger population of strong signals. This requires that all components in the RFD, especially preamplifiers, have sufficient dynamic

range to handle the total signal population collected over a desired frequency range. Eliminating the strong signals by attenuation, and other actions such as employing low-dynamic range preamplifiers, allowing site-generated EMI to seep into the RFD, and the use of RF components with limited shielding, simply blind the sites by preventing them from detecting the low-level signals of highest interest.

Some care is required in the interpretation of the results of the EMI leakage tests described in Section 3. For example:

- The tests were made with discrete-frequency test signals. Experience has show that EMI on conductors in a site consists of a combination of discrete-frequency spectral components and wide-band impulsive components.
- While the EMI current flowing on the conductors of a site generally decreases in amplitude with increasing frequency, exceptions to this general case do occur.
- There are deep nulls and peaks in the spectral shape of EMI current.
- Standing waves of EMI current and voltage exist on the conductors of a site.
- Leakage paths into the RFD appear to be, and probably are, frequency sensitive.

The combination of the two forms of EMI (discrete-frequency and impulsive), the erratic broadband spectral properties of EMI, and the complex nature of multiple leakage paths must all be considered. The complexity of the overall problem cannot be ignored. These factors complicate the analysis of the impact of leakage on the reception of radio signals. The formulation of a useful model describing the impact of EMI leakage on the operation of a receiving site is beyond today's system-modeling capability.

Discrete-frequency components of EMI current can be directly scaled in amplitude, and they can be expressed in terms of frequency-varying values of transfer impedance. However, the amplitude of the wide-band impulsive-noise portion of the EMI current changes with both measurement system and receiver bandwidth. This introduces an additional complication in the interpretation of the EMI leakage. First, the bandwidth of the EMI current measurement process must be considered since the true peak, rms, or average amplitude values are seldom provided by the measurement process. An amplitude-vs.-bandwidth function for each case of impulsive EMI must be established in order to determine its impact on the detection of signals. Fortunately, typical receiver bandwidths often limit the adverse impact of impulsive EMI on the signal-detection process of narrow-band signals. However, the signal-detection process is often

complicated by the limited linear operating range of most HF, VHF, and UHF receivers (20 to 30 dB when the RF gain is set at maximum) before AGC action starts suppressing weak signals. Many cases have been noted where leakage EMI is sufficiently strong that it, rather than the desired signal, operates the AGC and establishes the sensitivity and gain of the receiver.

4.2 Summary of Measured Leakage

It is of value to first examine the impact of the discrete-frequency spectral components of EMI current on RFD leakage. Table 4.2-1 organizes the measured results in order of leakage. The highest leakage results are placed on the first row of the table and decreasing leakage results on lower rows.

Table 4.2-1
Summary of Tolerable Levels of Discrete-frequency EMI Current

Injection Location	Maximum Tolerable LB EMI Current µA	Maximum Tolerable HB EMI Current µA
RG-85 Outside Term. Plate	362	50.1
MC Coax Inside Term. Plate	44.6	89
Pwr Panel Green Wire	8.9	0.7
Gnd Bus Under ENLARGER	1.3	0.8
WARS RF Cable Shield	0.25	0.3

The values of maximum EMI current provided in Table 4.2-1 are maximum leakage values obtained from the data. Average, quasi-peak, or other statistical values can be derived from the raw data. Due to the complexity of the leakage mechanisms, the complexity of the spectral structure of the actual EMI source current, the frequency-varying driving impedance of the conductors carrying EMI current, the unknown impact of inductive and capacitive coupling paths, and some radiation of the EMI test signal, a more comprehensive analysis than the simple

process used to obtain the numbers in Table 4.2-1 seems an unnecessary exercise. The above numbers are sufficient to understand the full nature of the problem and its solutions.

The EMI current limits in Table 4.2-1 show that site equipment which injects EMI current into the conductors of a site near RF paths is the greatest problem. This means that all possible means should be taken to move EMI-generating devices out of the RF Room and out of all nearby rooms with conductors leading back to the RF Room. Physical and electrical isolation is a practical, although limited, mitigation action; often providing paths for the return of EMI current to its source before harmful levels of EMI current reach sensitive leakage points. There are limits to physical separation since EMI-generating equipment often cannot be moved far enough from RF cables and other conductors. Moving them outside an operations building and into nearby buildings raises the issue of direct radiation into a site's antennas.

The EMI current limits in Table 4.2-1 also show that EMI current introduced into external cable shields (e.g., antenna cables, communications cables, telephone cables, etc.) can be partly isolated from the interior of a building with a simple grounded barrier plate located at the external surface of a building. This same practice provides isolation in the reverse direction, and it also provides effective lightning protection for equipment in the building.

4.3 Transfer Impedance

Transfer impedance, the ratio of EMI current on a conductor to RFD output voltage, is a useful way to describe leakage into the RFD. It is normally expressed as

$$Z_t = \frac{E_{out}}{I_{in}}$$

where Z_t in the transfer impedance, E_{out} is the EMI voltage measured at the RFD output, and I_{in} is the injection current. Transfer impedance is a valuable way to assess the general electromagnetic-isolation integrity of an RFD system.

Values of transfer impedance can be obtained from the raw data collected for Tests 1 through 5. The input current is provided. The values of leakage amplitude in dBm used in this document were obtained by measuring test-signal power in a 50-ohm load. The output voltage can be derived from the leakage values by converting each value into watts and then using Ohm's law to obtain the equivalent voltage values.

While the data was obtained to provide values of transfer impedance, the conversion was not done. This is because it was an additional step not required to obtain the desired end product, the maximum tolerable value of EMI current. The test was configured to directly obtain the desired maximum tolerable EMI current values.

4.4 Corrective Actions

The data in Sections 2 and 3 provide insight into the magnitude of the coupling of internal EMI into the signal paths of a receiving site. In most receiving sites internally-generated EMI, leaking into the RF paths, is sufficient to cause harmful levels of radio interference to the reception of SOI. Yet, these levels were usually not high enough to adversely affect the reception of high-level signals, those of little interest. An evaluation of the impact of site-generated EMI must be directed at the reception of the signals of maximum interest rather than the high-level signals of no interest.

The impact of site-generated EMI on the reception of SOI can be reduced by two methods:

1. Increase the isolation between low-level RF signal paths and EMI current flowing on the conductors of a site.
2. Lower the EMI current on the conductors of a site to harmless levels.

The first approach requires that all possible means be taken to isolate RF paths from EMI current flowing on conductors in a site. This includes the use of double-shielded coaxial cable for all RF paths (already accomplished at most sites), strict quality controls on the assembly of connectors on the coaxial cables, the use only of high-grade coax connectors, and the use of shielding for all components in the RFD. Recent site improvement programs have used open circuit-board construction in RF paths, a technique that is not tolerable in any modern receiving site containing digital and power-switching devices. This one aspect of most present-day receiving sites renders them very susceptible to EMI problems.

The second approach requires that harmful levels of EMI current be prevented from flowing on cable shields, ground conductors, conduits, air-conditioning ducts, and all other conductors electrically connected to those listed. This can only be accomplished by the correct

use of electromagnetic barriers at each item of equipment that injects harmful levels of EMI current into a site's conductors. Effective electromagnetic barriers can reduce the EMI current injected into the conductors of a site to harmless levels at low cost when properly done. Improperly done, they can be both expensive and ineffective. It is beyond the scope of this report to fully describe such electromagnetic barriers.

A third approach to the control of internally-generated EMI—the better grounding of equipment and systems—is often suggested. This approach is not effective and will not aid in the control or mitigation of internally-generated EMI problems. Better site grounds often provide lower impedance paths for the flow of EMI current, higher levels of standing waves, and increased coupling into RF paths. While improved facility and earth ground systems are often recommended, and they are required for personnel and equipment safety reasons, they will not help control EMI from internal sources.

In actual practice, a combination of the two effective control techniques listed above is the best approach. Care must be taken to insure the maximum possible leakage integrity of the RFD of all receiver sites. Equipment that injects harmful levels of EMI current into the conductors of a site must not be accepted, or it must first be modified to reduce the injected EMI current to tolerable levels.

4.5 Other Considerations

The introduction of EMI into low-level signal paths of the RFD from current flowing on cable shields, grounds, power conductors, and other conductors occurred by direct leakage into the site's RFD at the Wahiawa site. Direct radiation from EMI current flowing on conductors into the antenna has been identified at several small receiving sites. This additional mode of EMI is the primary problem at some small sites (e.g., Reference 2), and it has been found at some larger sites. Care must be taken to include direct radiation as a possible mode at all sites.

5. CONCLUSIONS

The EMI leakage tests described in this document show that present site-design procedures, equipment-installation practices, and site-maintenance techniques result in unacceptable levels of radio interference from sources located within a site. There are two reasons for this unfortunate conclusion.

The first reason is the relaxation of the isolation integrity of the RF paths by eliminating the complete shielding of all RF components. Examples of this are the open and unshielded circuit-boards now found in the RF paths of many sites, the use of single-shielded coaxial cable for RF paths, the use of improper coaxial connectors, and the use of unskilled personnel to assemble coaxial cables.

The second reason is the introduction of digital equipment and power-control equipment into receiving sites without adequate limits on the EMI current they inject into the conductors of a site. Examples include the use of standard UPS systems designed only for use in commercial installations that can tolerate larger levels of EMI current, the use of open shields on communications cables, the use of insulated coaxial bulkhead connectors on digital equipment, and the improper connection of cable shields into the interior of digital equipment.

This unfortunate state can be directly traced to the lack of suitable technical guidelines for the purchase of equipment, the installation of modern digital equipment and systems, and the maintenance of existing and new systems. Existing guidelines are a mixture of old material which is not applicable to present day receiving sites and old material that is based on solid technical concepts and is still useful; they generally lack the technical information needed to cope with the introduction of the new digital and power-control devices now available.

Without change, this unfortunate state will continue to get worse. New digital equipment and new power-control equipment employ ever increasing data bandwidths, clock rates, and shorter switching times to provide improved operational capabilities. Means are needed to fully take advantage of these improvements without jeopardizing the site's mission.

Today's EMI problems can be corrected at low cost over time without interrupting existing systems or procuring new systems. It only requires that the technical information needed to define site changes be prepared and used.

Appendix A

PERSONNEL

PERSONNEL

The WAH9607A team consisted of individuals from a number of government, educational, and commercial organizations. Each team member had prior experience with SNEP team surveys, the instrumentation used, and technical expertise needed to accomplish assigned tasks. The team members were:

Name	Organization
Hugh J. Myers	NRaD Activity Pacific
Jerry C. Cabradilla	NRaD Activity Pacific
Lester J. Chong	NRaD Activity Pacific
Arthur A. Kluvo	NRaD Activity Pacific
William A. Briotta	E-Systems, Falls Church
George F. Munsch	Consultant
Wilbur R. Vincent	Naval Postgraduate School
Richard W. Adler	Naval Postgraduate School

The team is grateful for the encouragement and assistance of the Commanding Officer, Captain Fishburne, the Department Head, LCDR Vulcan, and the OPS Officer, WO Springdale. LT Morgan, the electronics maintenance officer, assisted in the planning of the effort and in the implementation of the work described in this document. They cheerfully provided site personnel to aid in all aspects of the work.

The following site personnel aided the team on a daily basis, and they cheerfully assisted in the completion of the measurements described.

CTMC	Jenning (MAT Shop Chief)
RMC	Keppler (SPECOM Chief)
CTM1	Bollman
CTM1	Gustmite

We are also grateful for the help of the entire NSGD Honolulu CDAA staff. The conduct of this investigation interrupted their daily routine due to the need for a total power shutdown, frequent requests to turn off and on systems, equipment, and lights, and allowing us to poke around the site in an attempt to identify sources of radio interference.

INITIAL DISTRIBUTION LIST

		No. Copies
1.	Defense Technical Information Center 8725 John J. Kingman Rd, STE 0944 Ft. Belvoir, VA 22060-6218	2
2.	Dudley Knox Library, Code 52 Naval Postgraduate School 411 Dyer Road Monterey, CA 93943-5101	2
3.	Research Office, Code 09 Naval Postgraduate School 589 Dyer Road Monterey, CA 93943-5138	1
4.	Chairman, Code EC Department of Electrical and Computer Engineering Naval Postgraduate School 833 Dyer Road Monterey, CA 93943-5121	1
5.	Professor Richard W. Adler, Code EC/Ab Department of Electrical and Computer Engineering Naval Postgraduate School 833 Dyer Road Monterey, CA 93943-5121	10
6.	Professor Wilbur R. Vincent, Code EC/Ab Department of Electrical and Computer Engineering Naval Postgraduate School 833 Dyer Road Monterey, CA 9394-5121	10
7.	Mr. Robert M. Perry, Code EC/Ab Department of Electrical and Computer Engineering Naval Postgraduate School 833 Dyer Road Monterey, CA 93943-5121	1

		No. Copies
8.	CDR Gus Lott, Code EC/Lt Naval Postgraduate School 833 Dyer Road Monterey, CA 93943-5121	1
9.	Commander, Code N44 Naval Security Group Attn: Mrs. Jackie Sherry 9800 Savage Road Ft. Meade, MD 20755-6000	15
10.	Raytheon E-Systems Attn: Mr. Roy Bergeron 7700 Arlington Blvd. Falls Church, VA 22046	4
11.	USA INSCOM Attn: Ms. Anne Bilgihan IALD-MSA-SE Ft. Belvoir, VA 22060-5246	2
12.	NISE EAST Attn: Mr. James Engles 4600 Marriott Drive North Charleston, SC 29406	1
13.	NISE EAST Attn: Mr. Steve Kelly 4600 Marriott Drive North Charleston, SC 29406	1
14.	NISE EAST Attn: Ms. Pamela Guardabiged 4600 Marriott Drive North Charleston, SC 29406	1
15.	SRI International Attn: Mr. George Hagn 1611 No. Kent Street Arlington, VA 22209-2111	1

	No. Copies
16. Mr. George F. Munson Consultant 160 CR 375 San Antonio, TX 78253	1
17. NRaD Activity Pacific Attn: Mr. Brian Kutara 675 Lehua Avenue Pearl City, HI 96782-3356	5
17. NRaD Activity Pacific Attn: Mr. Hugh Myers 675 Lehua Avenue Pearl City, HI 96782-3356	1
18. Applied Research Laboratory Attn: Dr. Allan Sonstery Pennsylvania State University P.O. Box 30 State College, PA 16804	1